



## *Chapter 6*

# Existence of Exchange bias and Griffith Phase in $(\text{Tb}_{1-x}\text{Ce}_x)\text{MnO}_3$

## 6.1 Introduction

The study of  $RMnO_3$  ( $R = Gd, Tb, Dy, Ho$ ) is of considerable current interest owing to the co-existence of magnetic ordering and ferroelectricity with a strong coupling between them.<sup>1-5</sup> Moreover, a decrease in ionic radius of the  $R$  enhances the competition in magnetic interactions, i.e. ferromagnetic between nearest neighbouring Mn sites and anti-ferromagnetic between next nearest neighbouring sites.<sup>6</sup> The  $TbMnO_3$  is in the intermediate coupling region and as a matter of fact it is one of the most interesting materials<sup>7</sup> and has widely been studied.<sup>8-15</sup> This material shows antiferromagnetic ordering and ferroelectricity below 27K<sup>16</sup> and  $Mn^{3+}$  magnetic moments order  $\sim 41K$  ( $T_{N1}$ ) while  $Tb^{3+}$  magnetic moments order  $\sim 10 K$  ( $T_{N2}$ ). The frustrated spiral spin order of  $Mn^{3+}$  in  $TbMnO_3$  is thought to be the origin of ferroelectricity.<sup>17</sup> This intermediate coupling regime is very sensitive to any variation in  $J_{Mn-R}$  (exchange interaction between manganese and rare-earth ions) which strongly affects the Tb-magnetic ordering as has been observed by Prokhnenko *et al.*<sup>18</sup>

Moreover, in recent years, multifunctional materials have attracted valuable interest due to the coexistence of more than two properties simultaneously in one material e.g. multiferroicity, exchange Bias (anisotropy in hysteresis loop), Griffiths phase (inhomogeneity in spin ordering) etc. Many intrinsic multifunctional materials have been discovered and many artificially created by mixing two or more than two materials (like composites) or substituting some species of parent compound. The phenomenon of exchange anisotropy or bias (EB) is typically associated with a shifting of the hysteresis loop (Exchange-bias field,  $H_E$ ), measured after field-cooling, of a ferromagnetic (FM)-antiferromagnetic (AFM) interface through the Néel temperature  $T_N$  of the AFM component. These effects (EB) are applicable in the development of permanent magnets, magnetic recording media or domain stabilizers in recording heads based on anisotropic magnetoresistance and also in the reduction of the saturation fields to observe giant magnetoresistance (GMR) in exchange biased systems, as compared to standard GMR multilayer systems, which triggered a renewed interest in these phenomena.

Furthermore, the observation of a Griffith's phase (GP) in a number of doped Perovskite manganite oxides has been reported and is quite interesting. According to Griffith's theory, there is always a finite probability of finding ferromagnetic (FM) clusters with randomly distributed spin [i.e., in paramagnetic (PM) state] in the

temperature range  $T_C < T < T_G$ , where  $T_C$  and  $T_G$  are Curie-Weiss temperature and Griffith's temperature, respectively. The Griffiths phase is characterized by the formation of FM clusters below  $T_G$ . These clusters are formed thermodynamically during cooling and nucleated by the intrinsic randomness, which cause inhomogeneous magnetic distribution in the sample. Nevertheless, Griffith phase was characterized by the downturn deviation from Curie-Weiss law behavior in  $\chi^{-1}$  as the temperature approaches to  $T_C$  from above.

In this chapter, we have reported the existence of both Exchange bias and Griffith phase in  $TbMnO_3$  and also discussed the enhancement of Griffith phase with hole doping (by doping Ce) in  $TbMnO_3$ .

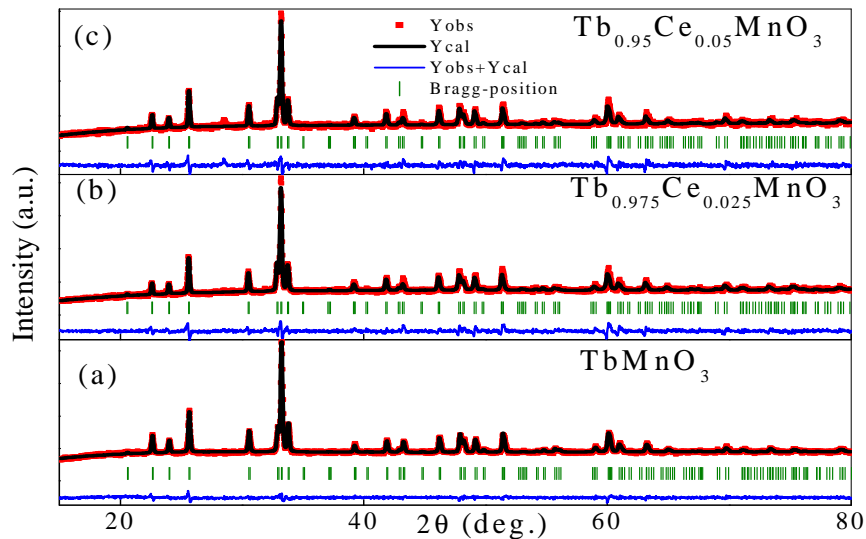
## 6.2 Experimental

The  $Tb_xCe_{1-x}MnO_3$  ( $x=0.0, 0.025, 0.05$ ) polycrystalline samples were synthesized by the conventional solid state reaction technique. Stoichiometric amounts of  $Tb_4O_7$ ,  $MnO$  (99.99% purity) and  $CeO_2$  were mixed and heated at  $1000^\circ C$  for 12 hours. The resulting powders were ground and pressed into pellets and sintered at  $1200^\circ C$  for 24 hours. The final step consisted on repressing and sintering the pellets at  $1300^\circ C$  for 48 hours with one intermediate grinding. Single phase of the samples were characterized by X-ray Diffractometer (Model: MiniFlex II, Rigaku, Japan) with  $Cu K\alpha$  radiation ( $\lambda=1.5406 \text{ \AA}$ ). Magnetic Measurement was done by SQUID (PPMS) magnetometer (Quantum Design).

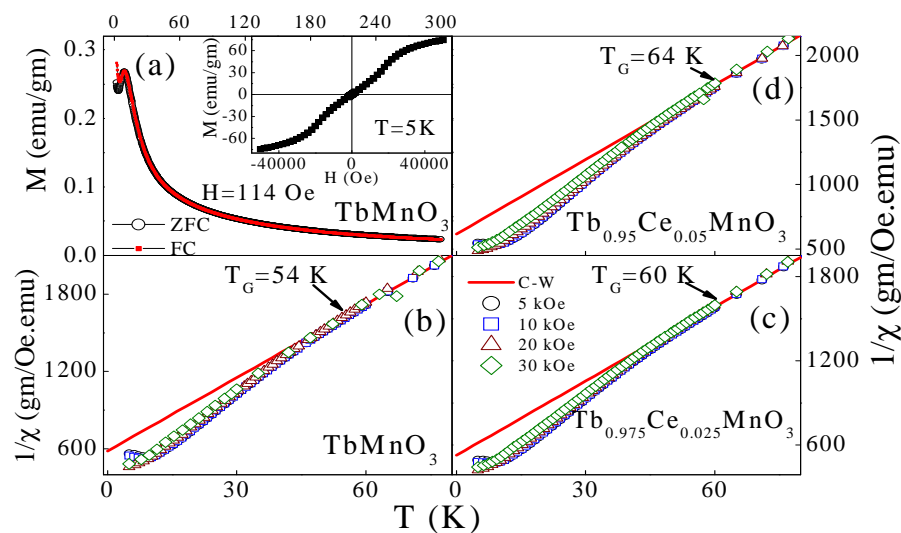
## 6.3 Result and Discussion

Fig. 6.1 shows XRD pattern of  $Tb_{1-x}Ce_xMnO_3$  ( $x=0.0, 0.025, 0.05$ ) which clearly indicates the single phase characteristics of polycrystalline  $TbMnO_3$  in orthorhombic structure with  $Pbnm$  space group. In Fig. 6.2 we have shown the magnetization (both zero field cooled and field cooled) as a function of temperature of  $TbMnO_3$ . Figure 6.2 also shows the Curie-Weiss (CW) fitted curve to the inverse susceptibility  $1/\chi$  vs temperature (5K-80K) of  $TbMnO_3$ ,  $Tb_{0.975}Ce_{0.025}MnO_3$ ,  $Tb_{0.95}Ce_{0.05}MnO_3$  under different cooling field 5 kOe, 10 kOe, 20 kOe, 30 kOe respectively. The high temperature tail gives negative extrapolated temperature indicating that the dominant magnetic interaction is anti-ferromagnetic. Moreover, from fig. 6.2 it is clear that in the higher temperature region above 52 K magnetization

behavior obeys the Curie-Weiss (CW) law but below this temperature deviation of inverse susceptibility data from the CW fitted curve has been observed. This downturn of inverse susceptibility curve indicates existence of different magnetic phases as FM, AFM, and PM below 52K.<sup>19-21</sup> This type of behavior below some temperature  $T_G$  (52K) but above  $T_C$  is defined as Griffith phase which is attributed to the formation of FM cluster embedded in AFM and PM region as observed in inhomogeneous magnetic layers of different materials.<sup>22</sup>



**Figure 6.1:** Reitveld refinement of XRD pattern of  $TbMnO_3$ ,  $Tb_{0.975}Ce_{0.025}MnO_3$ ,  $Tb_{0.95}Ce_{0.05}MnO_3$  respectively 6.1 (a, b, c).



**Figure 6.2:** Figure 6.2(a) shows Magnetization vs Temperature of  $TbMnO_3$  in the range of 2K – 300K at 114 Oe (Inset figure shows M-H curve of  $TbMnO_3$  at 5K). Figure 6.2 (b, c, d) shows Curie-Weiss (CW) fitted curve of inverse susceptibility  $1/\chi$  vs temperature (5K-80K) of  $TbMnO_3$ ,  $Tb_{0.975}Ce_{0.025}MnO_3$ ,  $Tb_{0.95}Ce_{0.05}MnO_3$  under different cooling field 5 kOe, 10 kOe, 20 kOe, 30 kOe respectively.

Moreover, it has been observed that the materials exhibiting GP usually give a much larger effective spin  $S_{eff}$ , deduced from the slope of the Curie–Weiss fitting on the high-T magnetization, than the value for an effective Mn ion<sup>21</sup> due to the contribution of individual entities containing more than two ions, i.e., FM clusters, in the high-T PM phase. In our case, we also evaluate the values of  $S_{eff}$  as  $10.51\mu_B$ ,  $10.9\mu_B$  and  $10.41\mu_B$  for  $TbMnO_3$ ,  $Tb_{0.975}Ce_{0.025}MnO_3$  and  $Tb_{0.95}Ce_{0.05}MnO_3$  respectively and we also calculated these values theoretically as  $8.48\mu_B$ ,  $8.43\mu_B$  and  $8.36\mu_B$  respectively. It is observed that these values are much larger than  $S_{eff}$  calculated theoretically. As discussed above there is a signature of Griffith phase in  $TbMnO_3$  indicating the possibility of existence of weak ferromagnetism. It is also observed that as the Ce content increases the Griffith phase also increases. It is well known that for a system with the Griffith Phase the downturn can be suppressed on increasing the external field due to polarization of spins outside the clusters. M-H curve of  $TbMnO_3$  at  $T=5K$  under field cooling FC (0 kOe, 10 kOe, 20 kOe, 30 kOe) is shown in figure 3. The isothermal magnetization data at 5K for  $TbMnO_3$  indicates a metamagnetic transition at 1.7 T (inset of Fig.6.2), which can be attributed to the magnetic reversal of Ising  $Tb^{3+}$  moments, as previously observed in both polycrystalline and single crystal  $TbMnO_3$ .<sup>23,24</sup> From figure 6.3 it is clear that on increasing FC (field cooling) coercivity of MH loop increases and also origin of hysteresis loop is shifted. This shows that exchange bias phenomena in  $TbMnO_3$  system exist as found in bilayers or multilayer magnetic systems and thin film<sup>25</sup>. It is well known that exchange bias effect is attributed due to inhomogeneous magnetic ordering in magnetic materials e.g. multilayer of AFM and FM.

So far no report is available regarding the existence of Griffith phase and Exchange bias in  $TbMnO_3$ . Rubi et al. have shown the ferromagnetic like interaction below the bulk Neel temperature<sup>26</sup> in  $TbMnO_3$  thin film. They have proposed the coupling between magnetization and strain as the origin of ferromagnetism. Recently, O'Flynn et al. have reported the bifurcation between ZFC and FC magnetization in  $TbMnO_3$  single crystal.<sup>27</sup> In the present investigation it may be suggested that the oxygen vacancy may be the origin of ferromagnetism which in effect leads to the Griffith phase. To verify this prediction we have carried out the energy dispersive X-ray (EDX) analysis of the  $TbMnO_3$  sample. It is clear from the figure 6.4 that some Oxygen vacancy is there. This Oxygen vacancy leads to convert some  $Mn^{3+}$  into  $Mn^{2+}$ .

Existence of these mixed  $2+/3+$  states may induce ferromagnetism<sup>28</sup>. In order to support this we have also doped Ce in the Tb site of  $TbMnO_3$  and synthesized  $Tb_{0.975}Ce_{0.025}MnO_3$  and  $Tb_{0.95}Ce_{0.05}MnO_3$  samples. The magnetic properties of these samples have also been shown in Figs.6.2 and 6.3.

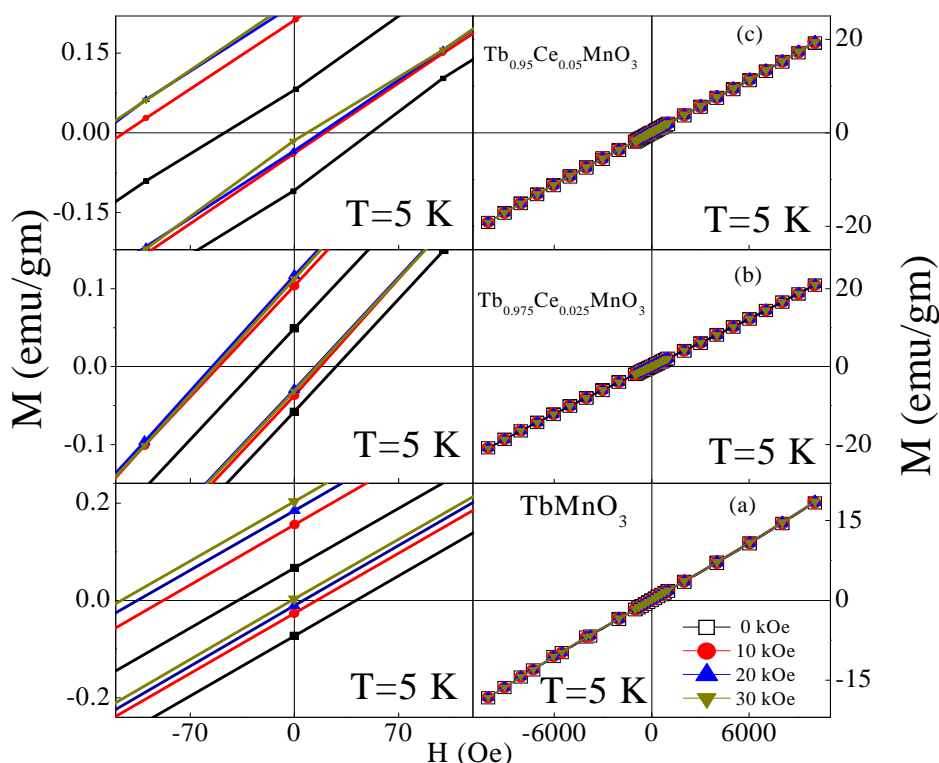


**Figure 6.3:** Figure 6.3(a, b, c) shows M-H curve of  $TbMnO_3$ ,  $Tb_{0.975}Ce_{0.025}MnO_3$ ,  $Tb_{0.95}Ce_{0.05}MnO_3$  at 5K and left side figure indicate extended view of these figures clearly indicates Exchange bias effect respectively.

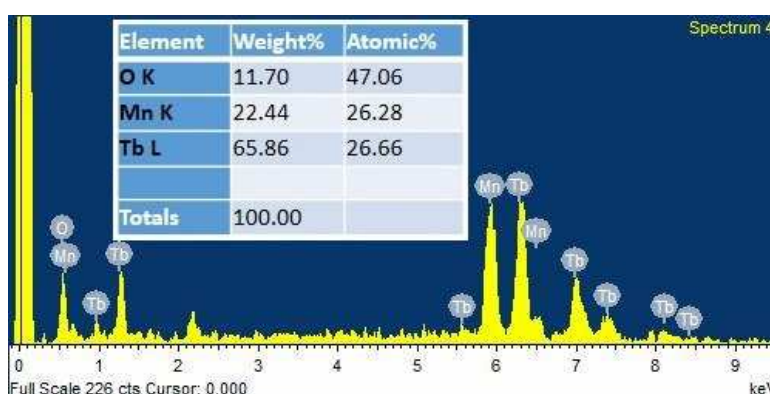


**Figure 6.4:** EDX spectra of  $TbMnO_3$ .

It is observed that both the samples show the Exchange bias and Griffith phase. Ce doping in  $TbMnO_3$ , which exists in the tetravalent ( $Ce^{4+}$ ) state, might be driving some of the  $Mn^{3+}$  ions into a  $Mn^{2+}$  state.<sup>28</sup> Exchange interaction between  $Mn^{3+}$  and

$Mn^{2+}$  is inducing ferromagnetism in  $TbMnO_3$  which might be the origin of Griffith phase observed in  $TbMnO_3$  and Ce doped  $TbMnO_3$ . Moreover, the Ce doping also changes the Mn-O-Mn angle (shown in Table 6.1) which in effect induce the canted anti-ferromagnetic ordering<sup>29</sup> in  $TbMnO_3$  and this canted AFM might be the origin of exchange bias in these materials.

**Table 6.1:** Reitveld refinement lattice parameter, Mn-O-Mn bond angle and Griffith temperature ( $T_G$ ) and Curie Temp. ( $T_C$ ) calculated by CW (Curie-Weis) fitting of inverse magnetic susceptibility vs Temperature of  $TbMnO_3$ ,  $Tb_{0.975}Ce_{0.025}MnO_3$ ,  $Tb_{0.95}Ce_{0.05}MnO_3$ .

Sample→ Parameters ↓	$TbMnO_3$	$Tb_{0.975}Ce_{0.025}MnO_3$	$Tb_{0.95}Ce_{0.05}MnO_3$
a (Å)	5.3029(2)	5.3112(3)	5.3096(3)
b (Å)	5.8458(2)	5.8570(3)	5.8503(4)
c (Å)	7.4094(2)	7.4192(4)	7.4195(4)
$T_G$ (Griffith Temp.) K	54	60	64
$T_C$ (Curie Temp.) K	-30.76	-29.87	-31.70
Mn-O <sub>1</sub> -Mn (deg.)	144.4 (6)	158.0 (4)	151.6 (4)
Mn-O <sub>2</sub> -Mn (deg.)	144.9 (5)	167.5 (5)	157.0 (4)

## 6.4 Conclusion

In summary, we have investigated the magnetic properties of  $Tb_{1-x}Ce_xMnO_3$  ( $x=0.0, 0.025, 0.05$ ). The undoped sample showed the existence of both exchange bias and Griffith phase. The Griffith phase has been attributed to the Oxygen vacancy which converts some  $Mn^{3+}$  states to  $Mn^{2+}$  states. The exchange interaction between  $Mn^{3+}/Mn^{2+}$  induces ferromagnetism. Furthermore, Ce doping also converts some  $Mn^{3+}$  states to  $Mn^{2+}$  states. As a consequence, Ce doped  $TbMnO_3$  also show Griffith phase. Moreover, The Oxygen vacancy/ $Mn^{3+}$ - $Mn^{2+}$  may change the Mn-O-Mn angle which in effect induces the canted AFM ordering. The canted AFM might be the origin of exchange bias.

**References:**

- <sup>1</sup>S.-W. Cheong and M. Mostovoy, *Nature Mater.***6**, (2007).
- <sup>2</sup>M. Pekala, V. Drozd, J. F. Fagnard, Ph. Vanderbemden and M. Ausloos, *J. Alloys Compounds***467**, 35 (2009).
- <sup>3</sup>T. Kimura, T. Goto, H. Shintani, K. Ishizaka, T. Arima and Y. Tokura, *Nature***426**, 55 (2003).
- <sup>4</sup>T. Goto, T. Kimura, G. Lawes, A. P. Ramirez and Y. Tokura, *Phys. Rev. Lett.***92**, 257201 (2004).
- <sup>5</sup>B. Lorenz, Y.-Q. Wang and C.-W. Chu, *Phys. Rev. B* **76**, 104405 (2007).
- <sup>6</sup>H. D. Zhou, J. C. Denyszyn and J. B. Goodenough, *Phys. Rev. B* **72**, 224401 (2005).
- <sup>7</sup>O. Prokhnenko, R. Feyerherm, M. Mostovoy, N. Aliouane, E. Dudzik, A. U. B. Wolter, A. Maljuk, and D. N. Argyriou, *Phys. Rev. Lett.* **99**, 177206 (2007).
- <sup>8</sup>M. Pekala, V. Drozd, J. F. Fagnard, Ph. Vanderbemden and M. Ausloos, *J. Alloys Compounds* **467**,35(2009).
- <sup>9</sup>Y. Y. Guo, Y. J. Guo, N. Zhang, L. Lin and J.-M. Liu, *Appl. Phys. A* **106**, 113(2012).
- <sup>10</sup>P. Rovillain, M. Cazayous, Y. Gallais, A. Sacuto, M.-A. Measson and H. Sakata *Phys. Rev. B* **81**, 054428 (2010).
- <sup>11</sup>F. W. Fabris, M. Pekala, V. Drozd, J. F. Fagnard, Ph. Vanderbemden, R. S. Liu and M. Ausloos, *J. Appl. Phys.* **101**, 103904 (2007).
- <sup>12</sup>J. Blasco, C. Ritter, J. Gorcia, J. M. de-Teresa, J. Perez-Cacho and M. R. Ibarra, *Phys. Rev. B* **62**,5609 (2000).
- <sup>13</sup>T. Goto, Y. Yamasaki, H. Watanabe, T. Kimura and Y. Tokura, *Phys. Rev. B***72**, 220403 (2005).
- <sup>14</sup>N. Mufti, A. A. Nugoroho, G. R. Blake and T. T. M. Palstra, *Phys. Rev. B* **78**, 024109 (2008).
- <sup>15</sup>D. O. Flynn, C. V. Tomy, M. R. Lees, A. Daoud-Aladin and G. Balakrishnan, *Phys. Rev. B***83**, 174426 (2011).
- <sup>16</sup>T. Kimura, T. Goto, H. Shintani, K. Ishizaka, T. Arima and Y. Tokura, *Nature***426**, 55(2003).



- <sup>17</sup> M. Mostovoy, Phys. Rev. Lett. **96**, 067601 (2006).
- <sup>18</sup> O. Prokhnenko, N. Aliouane, R. Feyerherm, E. Dudzik, A. U. B. Wolter, A. Maljuk, K. Kiefer and D. N. Argyriou Phys. Rev. B **81**, 024419 (2010).
- <sup>19</sup> A. Paul and S. Mattauch, Appl. Phys. Lett. **95**, 092502 (2009).
- <sup>20</sup> S. M. Zhou, S. Y. Zhao, Y. Q. Guo, J. Y. Zhao and L. Shi., J. Appl. Phys. **107**, 033906 (2010).
- <sup>21</sup> T. W. Eom, Y. H. Hyun, J. S. Park, Y. P. Lee, V. G. Prokhorov, V. S. Flis and V. L. Svetchnikov, Appl. Phys. Lett. **94**, 152502 (2009).
- <sup>22</sup> V. N. Krivoruchko, Low Temp. Phys. **40**, 586 (2014).
- <sup>23</sup> M. Staruch, G. Lawes, A. Kumarasiri, L. F. Cotica, and M. Jain, Appl. Phys. Lett. **102**, 062908 (2013).
- <sup>24</sup> T. Kimura, T. Goto, H. Shintani, K. Ishizaka, T. Arima and Y. Tokura, Nature **426**, 55 (2003).
- <sup>25</sup> X. Martí, F. Sánchez, D. Hrabovsky, L. Fàbrega, A. Ruyter, J. Fontcuberta, V. Laukhin, V. Skumryev, M. V. García-Cuenca, C. Ferrater, M. Varela, A. Vilà, U. Lüders and J. F. Bobo, Appl. Phys. Lett. **89**, 032510 (2006).
- <sup>26</sup> D. Rubi, C. de Graaf, C. J. M. Daumont, D. Mannix, R. Broer, and B. Noheda, Phys. Rev. B **79**, 014416 (2009).
- <sup>27</sup> D. O'Flynn, M. R. Lees and G. Balakrishnan, J. Phys.: Condens. Matter **26**, 256002 (2014).
- <sup>28</sup> P. Raychaudhuri, S. Mukherjee, A. K. Nigam, J. John, U. D. Vaisnav, R. Pinto and P. Mandal, J. Appl. Phys. **86**, 5718 (1999).
- <sup>29</sup> M. Staruch, G. Lawes, A. Kumarasiri, L. F. Cotica, and M. Jain, Appl. Phys. Lett. **102**, 062908 (2013).